'Sausage-String' Patterns in Blood Vessels at High Blood Pressures

Preben Alstrøm[1], Victor M. Eguíluz[2], Finn Gustafsson[3], and Niels-Henrik Holstein-Rathlou[3]

[1]CATS, The Niels Bohr Institute, DK-2100 Copenhagen, Denmark
[2]Instituto Mediterráneo de Estudios Avanzados IMEDEA (CSIC-UIB), E-07071 Palma de Mallorca, Spain
[3]Department of Medical Physiology, The Panum Institute, DK-2200 Copenhagen, Denmark

December 16, 1998

Abstract

A new Rayleigh-type instability is proposed to explain the 'sausage-string' pattern of alternating constrictions and dilatations formed in blood vessels at high blood pressure conditions. Our theory involves the nonlinear stress-strain characteristics of the vessel wall, and provides predictions for the conditions under which the normal cylindrical geometry of a blood vessel becomes unstable. The theory explains key features observed experimentally, e.g. the limited occurrence of the sausage-string pattern to small arteries and large arterioles, and only in those with small wall-to-lumen ratios.

Approximately 10% of the population in Western societies has high blood pressure and roughly half recieve pharmacological treatment. Despite the development of potent blood pressure lowering drugs, elevated blood pressure remains a major risk factor for development of stroke and heart disease. While the underlying mechanisms in the vast majority of cases of high blood

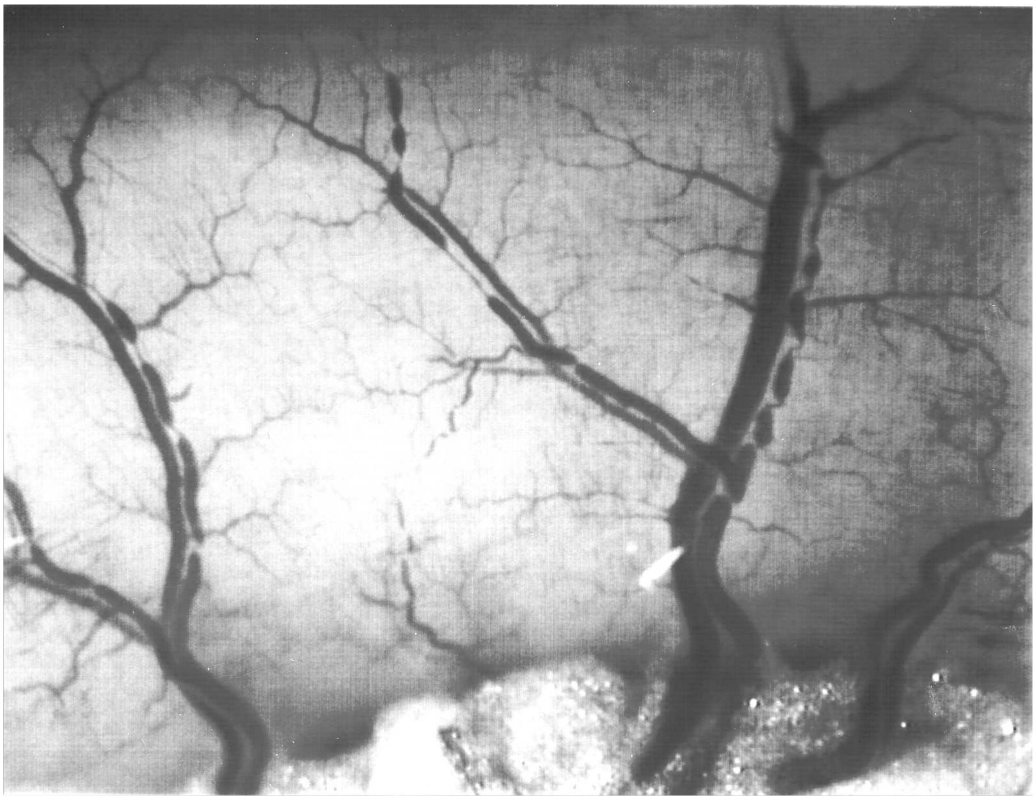

Figure 1: *In vivo* micrograph of rat intestinal arterioles showing a typical 'sausage-string' pattern following an acute increase in blood pressure induced by intravenous infusion of angiotensin II. The neighboring vessels not showing constrictions and dilatations are the corresponding venules. From [2].

pressure are unknown, it is clear that high blood pressure is primarily caused by an increase of resistance to blood flow in the circulation. This elevation in resistance to blood flow is induced by an increase in the tone of the small arteries and arterioles (diameter 30-300μ) by contraction of the smooth muscle cells surrounding the vessels. Smooth muscle cell contraction in arterioles and arteries may be induced by several vasoconstricting agents, one of the most potent being the octapeptide angiotensin II. Standard medication for high blood pressure includes drugs that lower the production or effects of vasoconstricting agents on the vascular smooth muscle cells.

Extreme increase in blood pressure, so-called malignant hypertension, may for example be encountered in patients with a kidney disease or in pregnant women suffering from preeclampsia. The underlying large increase in arterial resistance may be accompanied by severe damage to the circulatory system and result in organ dysfunction, particularly of the kidneys and the brain. This organ dysfunction may be irreversible and even fatal. In almost every case, malignant hypertension is accompanied - or caused - by considerable elevations of the blood levels of angiotensin II [1]. The vascular damage associated with substantial increase in blood pressure is confined to small arteries and arterioles, and it is preceded by a peculiar vascular reaction pattern: Initially extreme uniform narrowing of the blood vessels occurs. This is succeded by the development of alternating constriction and dilatation, giving the vessel a "sausage-string appearance" (Fig. 1). This vascular pattern has been demonstrated in many organs, including the brain, the gut, and the kidney [2] and it is of decisive importance to the subsequent development of vascular damage, since damage to the vascular wall occurs exclusively in the dilated regions of the vessel [3, 4, 5]. In the dilated segments, permeability to macromolecules from the blood stream is increased resulting in diffusion of proteins into the vessel wall. Presumably this in turn leads to local dysfunction and ultimatively death of the cells of the vascular wall.

In experimental studies of malignant hypertension in rats, high blood pressure is typically induced by intravenous infusion of angiotensin II [3, 4, 5]. As the infusion is continued, a substantial narrowing of the smaller blood vessels is observed, and at a given contraction, the narrowed vessels develop the sausage-string pattern (Fig. 1). Despite several decades of experimental research of the phenomenon, the mechanism causing the 'sausage-string' pattern has remained unknown [2]. It has been suggested that the pattern is caused by a 'blow out' of the vessel wall due to the high blood pressure [6], but this seems unlikely for several reasons. First, as mentioned above, the sausage-string pattern is observed only in the smaller vessels (small arteries and large arterioles), cf. Fig. 2, and here the pressure elevation is relatively small compared to that in the larger arteries. Secondly, the phenomenon is highly reproducible [4]. If the infusion of the vasoconstricting agent is stopped, the normal, uniform cylindrical geometry is restored without remaining deformations, as generally would be expected if the phenomenon was a breakdown due to mechanical failure of the elastic tissue. Restoring the infusion causes again an extreme, uniform vasoconstriction followed by the reappearance of the sausage-string pattern. A third and intriguing feature of the phenomenon is its overall periodicity with constrictions and dilatations occurring in a regular and repetitive pattern.

In this paper, we present a simple anisotropic, elastic model of the vessel wall. We show that under certain hypertensive conditions a novel Rayleigh-type instability occurs which leads to a periodic sausage-string pattern of constrictions and dilatations along the vessel. Our theory provides predictions for the conditions under which the cylindrical form of a blood vessel becomes unstable. Especially, we show that the appearance of the sausage-string pattern is limited to smaller blood vessels, because the pressure elevation there is relatively small (Fig. 2). Moreover, we show that the instability does not occur for vessels where the wall-to-lumen ratio (vessel-wall thickness divided by the inner radius) is large. In agreement herewith, the sausage-string pattern has not been observed in the small arterioles where the wall-to-lumen ratio is 0.3 - 0.5, compared to a value of 0.1 - 0.2 for larger blood vessels. Thus we argue that the sausage-string pattern is caused by an instability, and not by a mechanical breakdown. Furthermore, the borders of the instability window, where the sausage-string pattern appears, are determined by two different conditions, one related to the pressure, the other related to the geometry.

In order to investigate the stability of a cylindrically shaped blood vessel, consider an initial small axial symmetric perturbation of the inner radius, $r \to r + u(z)$ (Fig. 3). If the perturbation grows in time, the cylindrical form is unstable, if it decreases toward zero, the cylindrical form is stable. To determine the stability, we must therefore know the dynamic equation for the perturbation $u(z,t)$. To this end, we invoke the continuity equation,

$$\partial_t(\pi r^2) = -\partial_z J \ , \tag{1}$$

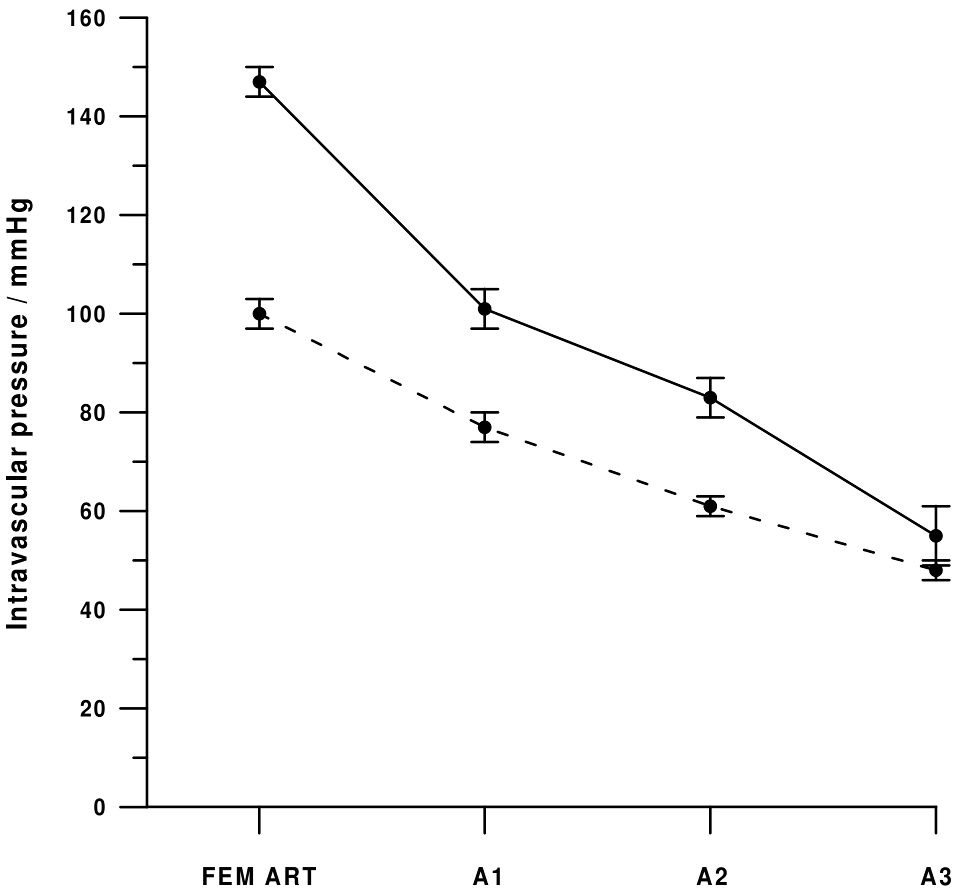

Figure 2: Intravascular pressure in a large (femoral) artery (FEM ART) of diameter ~ 1 mm, and in three categories of gut arterioles (A1-A3) in normal rats (dashed line) and rats with high blood pressure (solid line). Mean resting vessel diameters were: A1: 78 μm; A2: 30 μm; A3: 15 μm. From [7].

associating a local change of the cross-sectional area at a downstream site z with a fluid flux $J(z)$. The flux is related to the transmural pressure P, by

$$J = -c(r)\partial_z P \ , \tag{2}$$

where $c(r)$ is the vascular conductance. In the Hagen-Poiseuille approximation, the fluid conductance is $c(r) = \pi r^4/(8\eta)$, where η is the dynamic viscosity of the fluid (blood). However, the specific form of $c(r)$ is not crucial for our purpose.

¿From the continuity equation and the flux-pressure relation, the dynamic equation to lowest order in the perturbation follows,

$$\partial_t u = \frac{c(r)}{2\pi r}\partial_z^2 P \ . \tag{3}$$

Above, we have tacitly neglected the pressure drop along the vessel, noting that this is much smaller than the transmural pressure.

As a simple illustration, consider first a very thin vessel wall, for which the pressure is given by the Laplace form [8]

$$P = (T/R) + (T_z/R_z) \ . \tag{4}$$

Here T and T_z are the tensions circumferential to and parallel with the cylinder axis z, and $1/R$ and $1/R_z$ are the principal curvatures in the corresponding directions,

$$\frac{1}{R} = \frac{1}{r[1+(\partial_z r)^2]^{1/2}} \ , \quad \frac{1}{R_z} = \frac{-\partial_z^2 r}{[1+(\partial_z r)^2]^{3/2}} \ . \tag{5}$$

Furthermore, we assume that the tensions are constant and identical, $T_z = T$. Using the above expression, Eq. (4), for the pressure, we get from Eq. (3), retaining only linear terms in u,

$$\partial_t u = -\frac{Tc(r)}{2\pi r^3}[\partial_z^2 u + r^2\partial_z^4 u] \ . \tag{6}$$

For a perturbation of the form

$$u = \sum_k u_k(t)\cos(kz) \ , \tag{7}$$

(a)

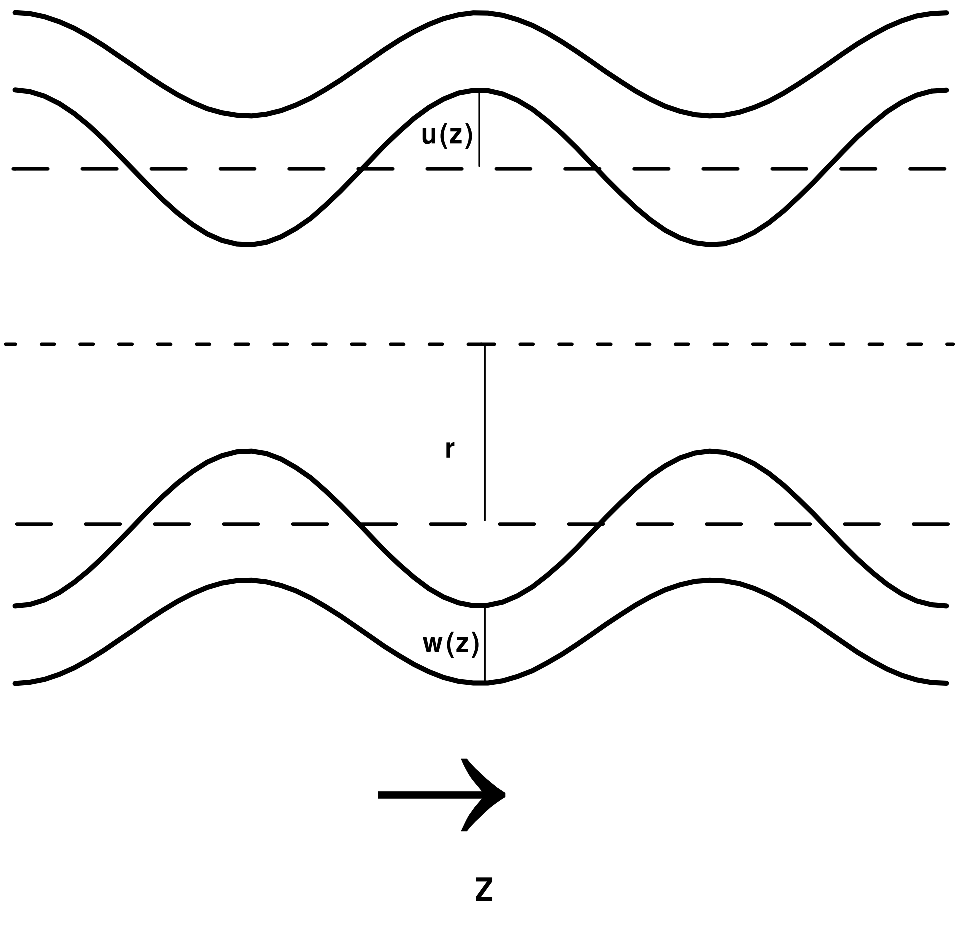

(b) (c)

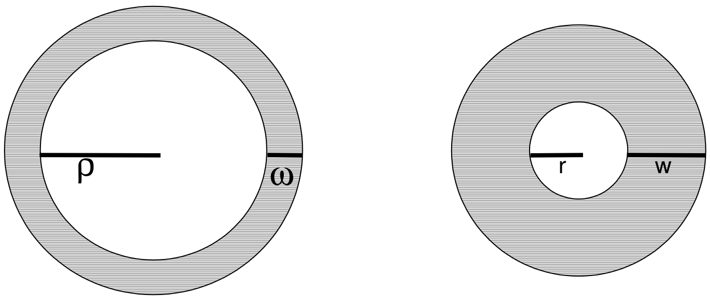

Figure 3: (a) A schematic picture of a blood vessel of inner radius r undergoing a perturbation $u(z)$. The wall thickness $w(z)$ is larger at smaller radii since the circumference is smaller. (b) Schematic cross-section of a blood vessel in relaxed state. (c) Schematic cross-section of a blood vessel in activated state. The cross-sectional area is assumed fixed, so the wall thickness is larger than in (b).

we have $u_k(t) \sim u_k(0)e^{\lambda_k t}$, where

$$\lambda_k = \frac{Tc(r)}{2\pi r^3}\, k^2[1 - r^2k^2] \; . \tag{8}$$

Thus, the vessel wall is unstable to modes with $rk < 1$. The dominant mode, where λ_k is maximal, is at $k = 1/(\sqrt{2}r)$.

The above instability is known as the Rayleigh instability [9, 10]. The theory explains why a cylindrical column of water with surface tension T is unstable at all radii. Alternatively, this can be shown in an energy context, varying the area

$$A = \int da = \int 2\pi r[1 + (\partial_z r)^2]^{1/2} dz \tag{9}$$

for fixed volume

$$V = \int \pi r^2 dz \; , \tag{10}$$

in order to minimize the suface energy

$$F = \int T da \; . \tag{11}$$

¿From a perturbation of the form $u = u_0 + u_k \cos(kz)$, where $u_0 = -u_k^2/(4r)$ [to lowest order in u_k] is determined by volume conservation, one obtains an energy change

$$\delta F = -F_0[1 - r^2k^2](u_k/2r)^2 \tag{12}$$

[to lowest order in u_k], which is again favorable (negative) when $rk < 1$.

The cylindrical geometry may remain stable if stabilizing terms appear in the energy functional F. In the recent analysis of the so-called pearling instability [11, 12], it is the reluctance against bending in tubular lipid membranes that stabilizes the cylindrical geometry. In the simplest form, an additional term [11]

$$\Delta F = \frac{1}{2}\kappa \int [\frac{1}{R} + \frac{1}{R_z}]^2 da \ , \tag{13}$$

κ being the bending modulus, is added to the surface energy. For Tr^2/κ sufficiently small, the cylindrical geometry remains stable (for all k). However, increasing the surface tension (using optical tweezers [11]), the instability occurs when Tr^2/κ crosses a given critical value.

In small blood vessels it is not the reluctance against bending but rather a strongly nonlinear stress-strain relation (Fig. 4) that is responsible for the stability of the cylindrical form. Under normal conditions, the stress is exponentially increasing with circumferential strain, and an increase in area by an amount δa is energetically much more expensive than gained by a similar decrease in area. Therefore, the cylindrical form remains stable. However, when the vessel contracts, the exponential behavior is replaced by a more slow variation, with a smaller area dependence in energy cost. At sufficiently strong contractions, energy is gained by reducing area, and the cylindrical form becomes unstable.

For blood vessels one cannot neglect the width w of the vessel wall. Taking the width of the vessel into account, the Laplacian form for the pressure is replaced by an integral,

$$P = \int_r^{r+w} [\ S \frac{1}{\tilde{r}[1 + (\partial_z \tilde{r})^2]^{1/2}} - S_z \frac{\partial_z^2 \tilde{r}}{[1 + (\partial_z \tilde{r})^2]^{3/2}}\ ]\ d\tilde{r} \ , \tag{14}$$

where S and S_z are the stresses, circumferential and parallel with the vessel. The stresses, S and S_z, defined as the forces per actual cross-sectional area, are related to the experimentally measured idealized stresses, σ and σ_z,

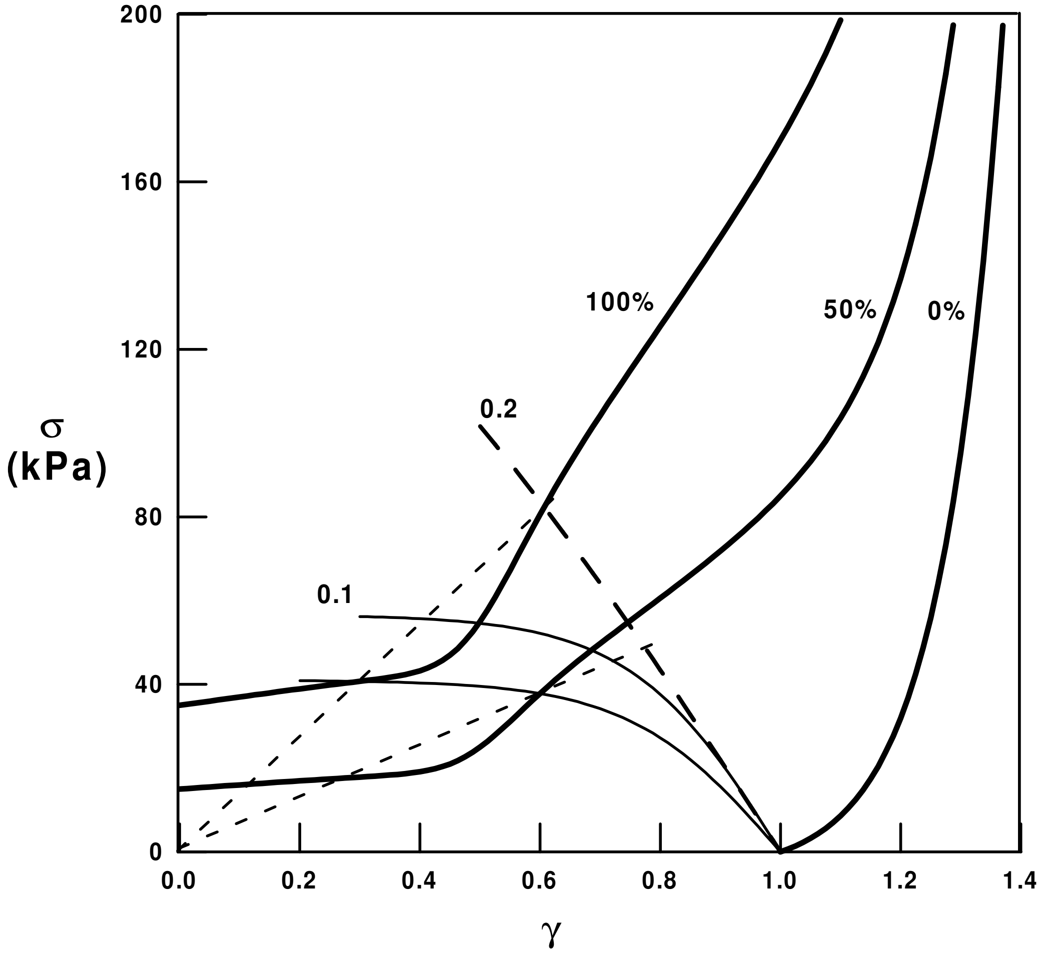

Figure 4: A schematic plot of typical stress-strain relations for arterioles (adapted from [13]). The three heavy solid curves correspond to a completely relaxed vessel (0%), a vessel where the smooth muscle cells are half maximally activated (50%), and a vessel where the smooth muscle cells are maximally activated (100%). The thin solid lines indicate how the points $(\gamma_r, \sigma(\gamma_r))$ and $(\gamma_w, \sigma(\gamma_w))$ [marked 0.1] move with muscle cell activation for an arteriole with wall-to-lumen ratio $\omega/\rho = 0.1$. The point of instability ($r = r_c$) for the cylindrical form of the blood vessel can be illustrated geometrically by thin dashed lines from $(0,0)$ through $(\gamma_r, \sigma(\gamma_r))$ [see text]. The instability point is where $\sigma(\gamma_w)/\gamma_w$ equals $\sigma(\gamma_r)/\gamma_r$. The thick dashed line [marked 0.2] shows how the point $(\gamma_w, \sigma(\gamma_w))$ move with muscle cell activation for an arteriole with $\omega/\rho = 0.2$, keeping the same curve for $(\gamma_r, \sigma(\gamma_r))$.

defined as the forces per relaxed cross-sectional area [14],

$$S = \gamma\gamma_z\sigma \ , \quad S_z = \gamma\gamma_z\sigma_z \ . \tag{15}$$

Here γ and γ_z are the normalized lengths in the circumferential direction and in the vessel direction, i.e. γ (γ_z) is equal to L/L_0 where L is the actual length of a tissue strip in the circumferential direction (vessel direction) and L_0 is the corresponding resting length. The strain, ϵ (ϵ_z), is by definition equal to $\gamma - 1$ ($\gamma_z - 1$). Since the length of a vessel remains almost constant during a contraction, γ_z is here assumed to be constant, $\gamma_z = \gamma_0$. Correspondingly, the stress σ_z is replaced by a constant σ_0.

The width w of the vessel wall changes when the inner radius r changes (Fig. 3). Assuming that the cross-sectional area of the vessel wall is constant, the radius dependence of w is given, when the inner radius ρ and wall thickness ω are known for the angularly relaxed state ($\gamma = 1$). We have

$$(r + w)^2 - r^2 = (\rho + \omega)^2 - \rho^2 \ . \tag{16}$$

Equation (16) suggests a useful change of variable, from $\tilde{r}$ to $\tilde{\rho}$, where

$$\tilde{r}^2 - r^2 = \tilde{\rho}^2 - \rho^2 \ . \tag{17}$$

When $\tilde{r}$ varies between values r and $r+w$, which under perturbations changes along the z axis, $\tilde{\rho}$ varies between the fixed values ρ and $\rho+\omega$. The normalized length γ at a radius $\tilde{r}$ is simply the ratio between $\tilde{r}$ and its relaxed value $\tilde{\rho}$: $\gamma = \tilde{r}/\tilde{\rho}$ (Fig. 3).

For small perturbations, the relevant expression for the pressure reduces to

$$P = \gamma_0 \int_\rho^{\rho+\omega} [\sigma - \sigma_0 r \partial_z^2 r][\tilde{\rho}^2 - \rho^2 + r^2]^{-1/2} \, d\tilde{\rho} \ , \tag{18}$$

where the stress σ in the circumferential direction depends on the normalized length

$$\gamma = [\tilde{\rho}^2 - \rho^2 + r^2]^{1/2}/\tilde{\rho} \ . \tag{19}$$

To linear order in the perturbation $u(z,t)$, we obtain

$$P = P_0(r) + I(r)u - I_0(r)\partial_z^2 u \ , \tag{20}$$

where

$$P_0(r) = \gamma_0 \int_\rho^{\rho+\omega} \sigma[\tilde\rho^2 - \rho^2 + r^2]^{-1/2}\, d\tilde\rho \ , \tag{21}$$

$$\begin{aligned} I_0(r) &= \gamma_0\sigma_0 r \int_\rho^{\rho+\omega} [\tilde\rho^2 - \rho^2 + r^2]^{-1/2}\, d\tilde\rho \\ &= \gamma_0\sigma_0 r \log[1 + (\omega + w)/(\rho + r)] \ , \end{aligned} \tag{22}$$

and

$$I(r) = \frac{d}{dr}P_0(r) = \gamma_0 \int_\rho^{\rho+\omega} \tilde\rho^{-1} \frac{d}{d\gamma}\left[\frac{\sigma}{\gamma}\right] \frac{\partial\gamma}{\partial r}\, d\tilde\rho \ . \tag{23}$$

The partial derivatives of γ with respect to r and $\tilde\rho$ are related,

$$\tilde\rho^{-1}(\partial\gamma/\partial r) = r(\rho^2 - r^2)^{-1}(\partial\gamma/\partial\tilde\rho) \ , \tag{24}$$

and $I(r)$ can be expressed in terms of the normalized length γ,

$$I(r) = \frac{\gamma_0\gamma_r}{\rho(1-\gamma_r^2)}\left[\frac{\sigma(\gamma_w)}{\gamma_w} - \frac{\sigma(\gamma_r)}{\gamma_r}\right] \ , \tag{25}$$

where

$$\gamma_r = r/\rho \ , \quad \gamma_w = (r+w)/(\rho+\omega) \ , \tag{26}$$

are the normalized inner and outer radius. Note that $I(r)$ is not singular at $\gamma_r = 1$, where also $\gamma_w = 1$.

By Eq. (20), the dynamic equation, Eq. (3), for the perturbation $u(z,t)$ takes the form

$$\partial_t u = -\frac{c(r)}{2\pi r}[-I(r)\partial_z^2 u + I_0(r)\partial_z^4 u] \ . \tag{27}$$

For a perturbation of the form (7), we have $u_k(t) \sim u_k(0)e^{\lambda_k t}$ with

$$\lambda_k = \frac{c(r)}{2\pi r}\, k^2[-I(r) - I_0(r)k^2] \ . \tag{28}$$

The value of $I_0(r)$ is always positive. Therefore, it is the sign of $I(r)$ that determines the stability of the vessel wall. If $I(r)$ is positive the cylindrical geometry is stable for all modes. If $I(r)$ is negative, the cylindrical geometry is unstable, more specifically to modes with $k^2 < |I|/I_0$.

The dominant (fastest growing) mode, where λ_k is maximal, is at the value $k = [|I|/(2I_0)]^{1/2}$, corresponding to 'sausages' of length

$$\ell = 2\pi[2I_0/|I|]^{1/2} \ . \tag{29}$$

For $\omega/\rho = 0.1$, and $\sigma_0 = 100$ kPa, we find $|I|\rho \approx 2I_0/\rho \approx 10$ kPa. Hence, $\ell \approx 2\pi\rho$, and the length of the 'sausages' will be 5-10 times the radius of the relaxed vessel. This is in good agreement with experimental observations [4] (Fig. 1).

¿From the expression for $I(r)$, Eq. (25), it is seen that the important quantity is σ/γ. The cylindrical form becomes unstable when σ/γ calculated at the inner radius ($r = r_c$) equals the value of σ/γ at the outer radius. This is illustrated geometrically (Fig. 4), by drawing a line (thin dashed) in the plot of σ versus γ from $(0, 0)$ through $(\gamma_r, \sigma(\gamma_r))$. The slope of this line is obviously $\sigma(\gamma_r)/\gamma_r$. If the point $(\gamma_w, \sigma(\gamma_w))$ lies above this line, $\sigma(\gamma_w)/\gamma_w > \sigma(\gamma_r)/\gamma_r$, $I(r)$ is positive, and the cylindrical form is stable. If on the other hand the point $(\gamma_w, \sigma(\gamma_w))$ lies below the line, $\sigma(\gamma_w)/\gamma_w < \sigma(\gamma_r)/\gamma_r$, $I(r)$ is negative, and the cylindrical form is unstable.

Under normal physiological conditions, the circumferential stress σ in blood vessels increases exponentially with the normalized length [8, 13] (Fig. 4), and the value of $I(r)$ is therefore positive (Fig. 5). This ensures that the blood vessel keeps its cylindrical form. However, when acute hypertension is induced by infusion of a strong vasoconstricting agent like angiotensin II, there will be a significant reduction of the inner radius in small arteries and large arterioles due to contraction of the smooth muscle cells. The operating point for the vessel will move to the less steep part of the $\sigma - \gamma$ curve (Fig. 4), and when the inner radius is reduced below a certain value r_c at which $\sigma(\gamma_w)/\gamma_w = \sigma(\gamma_r)/\gamma_r$, the value of $I(r)$ becomes negative (Fig. 5). The cylindrical form becomes unstable, and the 'sausage-string' pattern appears.

The 'sausage-string' pattern following infusion of angiotensin II has been found to occur predominantly in small arteries and large arterioles [4]. In accordance herewith, the present analysis predicts that large vessels will be stable. In this case, the operating point $(\gamma, \sigma(\gamma))$ lies on the steep part of the $\sigma - \gamma$ curve, at high pressure elevation and rather small contraction (Fig. 2 and Fig. 4), thus the larger vessels do not reduce their radii below the critical value r_c. As arterial vessels get smaller, the wall-to-lumen ratio ω/ρ generally increases [8]. From the expression for $I(r)$, Eq. (25), we find that

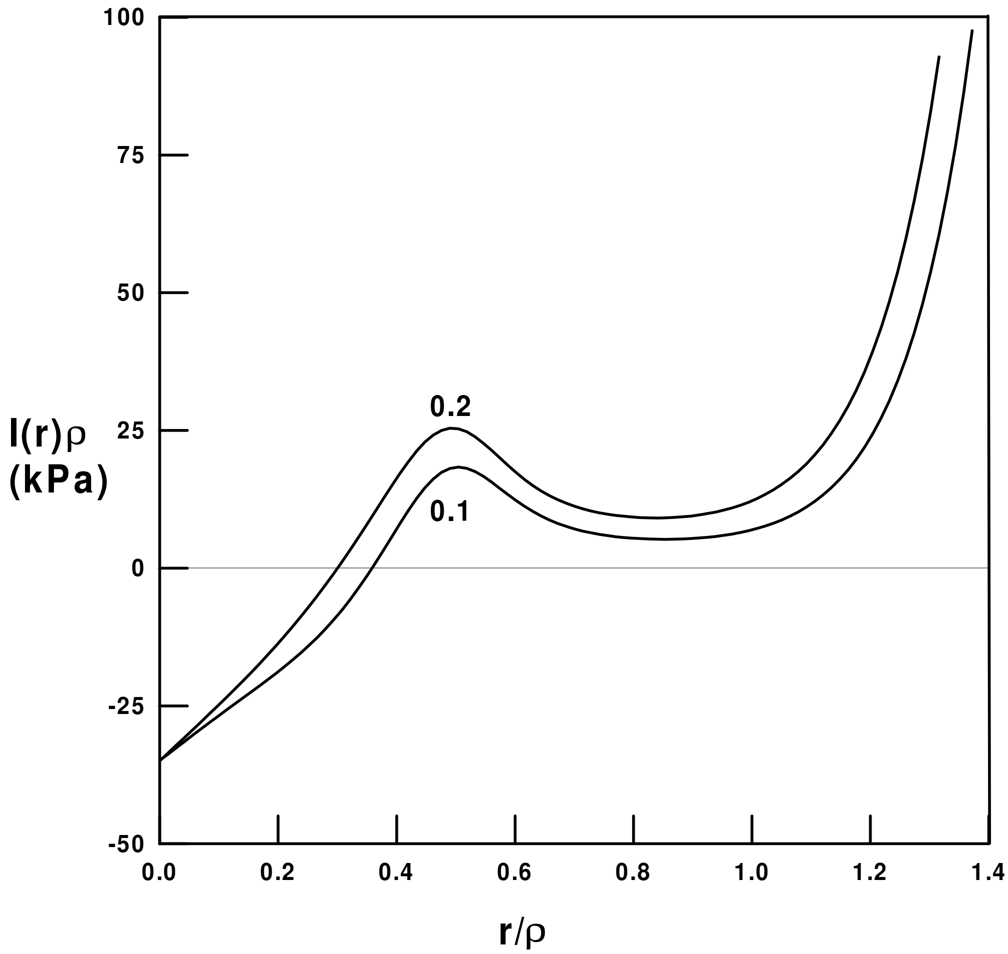

Figure 5: A plot of the stability measure $I(r)$ at large muscle cell activation for two different wall-to-lumen ratios, $\omega/\rho = 0.1$ and $\omega/\rho = 0.2$. The cylindrical form of a blood vessel becomes unstable when I becomes negative (at $r = r_c$). An almost linear stress-strain relation in a region above r_c gives rise to a decay of I. Above $\gamma = 1$, where the stress increases exponentially, also $I(r)$ increases exponentially.

the value of r_c decreases with increasing wall-to-lumen ratio ω/ρ (Fig. 6). In Fig. 4, the thin solid lines illustrate how the points $(\gamma_r, \sigma(\gamma_r))$ and $(\gamma_w, \sigma(\gamma_w))$ [marked 0.1] move with muscle cell activation for an arteriole with wall-to-lumen ratio $\omega/\rho = 0.1$. For a given activation of the smooth muscle cells (50%, 100%), a thin dashed line is drawn from $(0, 0)$ through $(\gamma_r, \sigma(\gamma_r))$. As argued above, when the point $(\gamma_w, \sigma(\gamma_w))$ lies above the thin dashed line, the cylindrical form is stable; when it lies below, the cylindrical form is unstable. For $\omega/\rho = 0.1$, we see from Fig. 4 that the cylindrical form is stable at 50% activation, but unstable at 100% activation of the smooth muscle cells surrounding the blood vessel. For $\omega/\rho = 0.2$ ($(\gamma_w, \sigma(\gamma_w))$ illustrated by thick dashed line marked 0.2), the cylindrical form is only barely unstable at 100% activation. For larger wall-to-lumen ratios, the cylindrical form remains stable (Fig. 6). Hence, the 'sausage-string' instability will not appear in blood vessels with large wall-to-lumen ratios. While the transmural pressure and the contractile potential sets an upper limit, the wall-to-lumen ratio sets a lower limit for vessels that will undergo the 'sausage-string' instability in response to an acute increase in blood pressure.

We note that when $I(r)$ becomes negative, the pressure at slightly larger radii is smaller than at slightly smaller radii. Accordingly, the resulting flow J will be directed from low-radii regions to high-radii regions, causing the small radii to become even smaller, and the large radii to become larger. This continues until the pressure stabilizes at a value which is the same for both the large radius r_{max} and the small radius r_{min}. The stabilization is possible because the pressure for radii above the instability, $r > r_c$, again increases with r. The theory allows an estimate of the radius in the dilated regions, r_{max}. Assuming that r_{min}/ρ is small (close to zero), the final value of r_{max} is estimated by the condition $P(r_{max}) = P(0)$. Interestingly, the almost linear stress function in the region above r_c (Fig. 4) gives rise to a decay of $I(r)$ in the same region (Fig. 5). As a consequence r_{max}/r_{min} can become quite large. However, close to $\gamma = 1$, the stress increases exponentially due to the elastic properties of the vessel wall [8], and the value of $I(r)$ will also increase rapidly. This will prevent r_{max} from attaining a value substantially larger than the relaxed radius, ρ, of the vessel. Preliminary experimental data from our laboratory confirm this. However, r_{max} may be larger than the working radius of the vessel under normal physiological conditions, because the normal working radius is smaller than the relaxed radius [8], i.e. the vessel has spontaneous tone. This may explain why earlier the dilated regions have

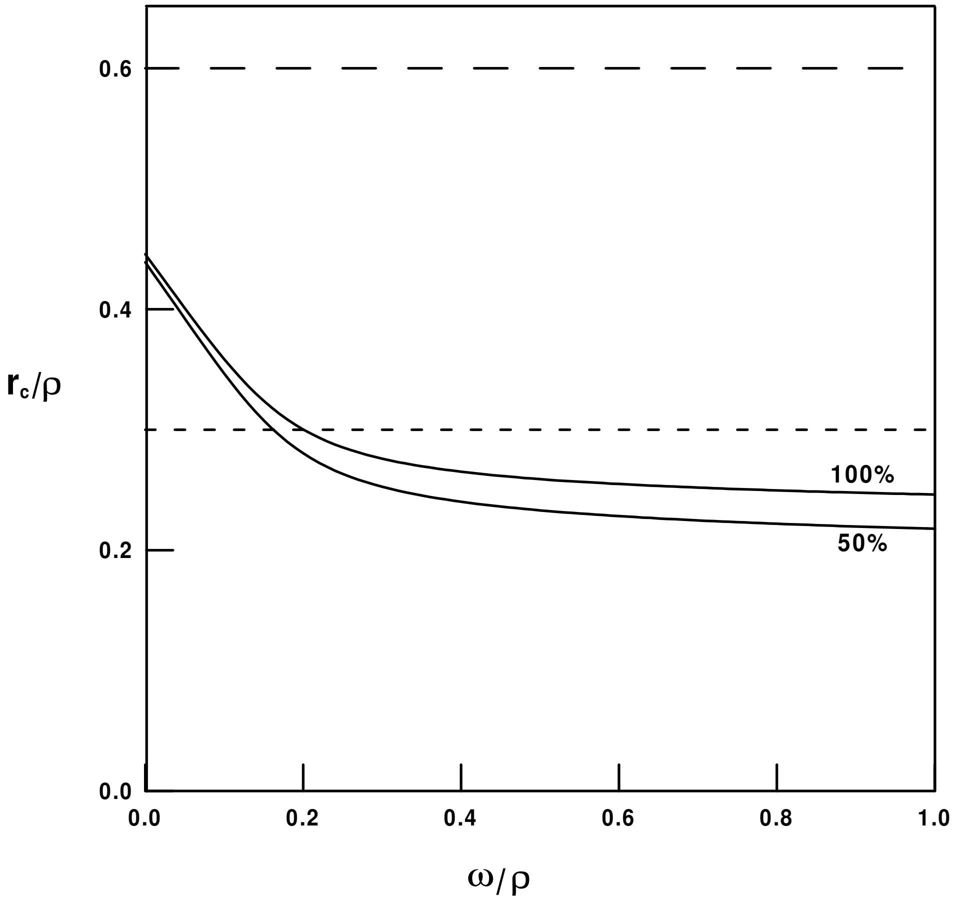

Figure 6: The critical radius r_c, normalized by relaxed radius ρ, decreases with (relaxed) wall-to-lumen ratio ω/ρ. Above the r_c curve, the cylindrical form is stable, below it is unstable. The dashed lines indicate the circumferential normalized lengths $\gamma_r = 0.6$ at 50% and $\gamma_r = 0.3$ at 100% activation of the smooth muscle cells. At 50% activation, the γ_r line lies entirely in the stable regime, and the cylindrical form is stable for all wall-to-lumen ratios. At 100% activation, the γ_r line lies in the unstable regime for wall-to-lumen ratios below 0.2, hence the cylindrical form is unstable for blood vessels with $\omega/\rho < 0.2$.

been suggested as a 'blow out' due to mechanical failure of the vessel wall [6].

In summary, we have demonstrated that during severe vasoconstriction, the normal cylindrical geometry of a blood vessel may become unstable, resulting in a sausage-string pattern of alternating constrictions and dilatations. The sausage-string pattern is thus the expression of an instability, and not caused by a mechanical failure of the vessel wall due to a high blood pressure. The instability is associated with the Rayleigh instability of a fluid column and with the 'pearling' instability observed in tubular lipid membranes. The mechanism behind the instability is however novel, involving the nonlinear stress-strain characteristics of the vessel wall. The developed theory explains many of the key features observed experimentally, especially why the instability is only observed in small arteries and large arterioles, and predominantly in those with small wall-to-lumen ratios.

The present study was supported by grants from the Danish Natural Science Research Council, the Danish Medical Research Council, and the Danish Heart Association.

References

[1] C. Kitiyakara and N.J. Guzman, J. Am. Soc. Nephrol. **9**, 133 (1998).

[2] F. Gustafsson, Blood Pressure **6**, 71 (1997).

[3] F. B. Byrom, Lancet **2**, 201 (1954); F.B. Byrom, Prog. Cardiovasc. Dis. **1**, 31 (1974).

[4] J. Giese, Acta Pathol. Microbiol. Scand. **62**, 497 (1964).

[5] J. Giese, *The Pathogenesis of Hypertensive Vascular Disease* (Munksgaard, Copenhagen, 1966).

[6] L.J. Beilin and F.S. Goldby, Clin. Sci. Mol. Med. **52**, 111 (1977).

[7] G. A. Meininger, K. L. Fehr, M. B. Yates, J. L. Borders, and H. J. Granger, Hypertension **8**, 66 (1986).

[8] Y.C. Fung, *Biomechanics. Mechanical Properties of Living Tissues, 2nd Ed.* (Springer-Verlag, New York, 1990); Y.C. Fung, *Biomechanics. Motion, Flow, Stress, and Growth* (Springer-Verlag, New York, 1990).

[9] J. Plateau, *Statique Experimentale et Theorique des Liquides Soumis aux Seules Forces Moleculaires* (Gautier-Villars, Paris, 1873).

[10] Lord Rayleigh, Philos. Mag. **34**, 145 (1892).

[11] R. Bar-Ziv and E. Moses, Phys. Rev. Lett. **73**, 1392 (1994).

[12] P. Nelson, and T. Powers, Phys. Rev. Lett. **74**, 3384 (1995); R.E. Goldstein, P. Nelson, T. Powers, and U. Seifert, J. Phys. II France **6**, 767 (1996).

[13] R.W. Gore, Circ. Res. **34**, 581 (1974); M.J. Davis, and R.W. Gore, Am. J. Physiol. **256**, H630 (1989).

[14] R. Feldberg, M. Colding-Jørgensen, and N.-H. Holstein-Rathlou, Am. J. Physiol. **269**, F581 (1995).